Electrical System Planning of Large-scale Offshore Wind Farm Based on *N*+ Design Considering Optimization of Upper Power Limits of Wind Turbines

Shurong Wei, *Member*, *IEEE*, Hao Wang, Yang Fu, *Member*, *IEEE*, Fangxing Li, *Fellow*, *IEEE*, and Lingling Huang, *Member*, *IEEE*

***Abstract*—Electrical system planning of the large-scale offshore wind farm is usually based on $N-1$ security for equipment lectotype. However, in this method, owing to the aggregation effect in large-scale offshore wind farms, offshore electrical equipment operates under low load for long periods, thus wasting resources. In this paper, we propose a method for electrical system planning of the large-scale offshore wind farm based on the *N*+ design. A planning model based on the power-limited operation of wind turbines under the *N*+ design is constructed, and a solution is derived with the optimization of the upper power limits of wind turbines. A comprehensive evaluation and game analysis of the economy, risk of wind abandonment, and environmental sustainability of the planned offshore electrical systems have been conducted. Moreover, the planning of an infield collector system, substation, and transmission system of an offshore electrical system based on the *N*+ design is integrated. For a domestic offshore wind farm, evaluation results show that the proposed planning method can improve the efficiency of wind energy utilization while greatly reducing the investment cost of the electrical system.**

***Index Terms*—Electrical system, *N*+ design, offshore wind farm, planning, optimization.**

I. Introduction

LARGE-SCALE generation of offshore wind power can notably contribute to achieving the goals of carbon peaking and carbon neutrality. With the release of "National Development and Reform Commission Notice on Improving the Feed-in Tariff Policy for Wind Power" in China, those newly approved onshore wind power projects after January 1, 2021 should fully achieve grid parity, and year-round trouble-free operation of wind farms has become a new goal for industrial development. On March 10, 2022, the construction of Shandong Energy Group Bozhong Offshore Wind Power A-Site Project, the first affordable offshore wind power project of China, officially began. This commencement marked the official entry of offshore wind power into the era of parity development, which increases the demand for cost reduction and efficiency. Electrical systems are costly, accounting for approximately 15%-30% of the total investment in an offshore wind farm [1]. With the development of large-scale clustered offshore wind power systems in the deep and distant sea, the electrical system investment can be substantially optimized while satisfying requirements and engineering constraints. Under the urgent demands of large-scale development and grid parity of offshore wind power, electrical system planning must be optimized.

Electrical system planning and optimization have been research hotspots in offshore wind power generation in recent years. Models of construction investment cost and reliability optimization considering the number of offshore wind farm cables and location and number of offshore substations have been developed with comprehensive evaluations of electrical network structures [2]-[5]. Considering the electromagnetic environment constraints of an electrical system, an optimization model combining environment, economy, and reliability has been developed [6], [7], and topology planning of a collector system under environmental constraints in two levels has been solved, thereby reducing the magnetic interference range in a wind farm. In [8], a bilevel multi-objective model has been built to configure wind turbines in offshore wind farms and optimize the topology of the collector system. In [9], coupling random fork tree coding, union-find set loop identification, and current/voltage drop calculation models have been developed, providing a basis for integrated design of a collector system. To avoid building planning models of complex power grid, uncertain planning models of transmis-

Manuscript received: October 12, 2022; revised: January 8, 2023; accepted: March 28, 2023. Date of CrossCheck: March 28, 2023. Date of online publication: May 1, 2023.

This work was supported by the National Natural Science Foundation of China (No. 51907115), the Major Natural Science Project of Shanghai Municipal Education Commission (No. 2021-01-07-00-07-E00122), the Shanghai Science and Technology Innovation Action Plan Project (No. 22dz1206100), and the Program for Professor of Special Appointment (Eastern Scholar) at Shanghai Institutions of Higher Learning (No. TP2020066).

S. Wei, H. Wang, Y. Fu (corresponding author), and L. Huang are with the Department of Electrical Power Engineering, Shanghai University of Electric Power, Shanghai 200090, China (e-mail: wsrmail@163. com; 244958540@qq. com; mfudong@126.com; linglinghuang82@126.com).

F. Li is with the Department of Electrical Engineering and Computer Science, The University of Tennessee, Knoxville, TN 37996, USA (e-mail: fli6@utk.edu).

DOI: 10.35833/MPCE.2022.000656

sion systems have been transformed into deterministic equivalent classes in [10], [11]. Then, traditional methods have been used to establish the corresponding planning models to facilitate modeling and solving. In [12], [13], numerical simulations of offshore wind power planning and investment strategic decision-making have been performed based on evolutionary game theory and interval intuitionistic fuzzy sets, respectively.

The abovementioned methods are based on the $N-1$ principle, in which the failure of any independent element among the N elements of a power system either causes line overload or leads to customer outages. The principle is widely used in conventional power system planning and design. With the large-scale deployment of offshore wind power, various remarkable characteristics appear. The aggregation effect of large wind farm clusters reduces the maximum output power, reaching approximately 90% of the installed capacity [14], [15]. On the other hand, according to statistics, the full power output time of typical offshore wind farms accounts for approximately 10% in a year, while the time of output power below 20% of the installed capacity accounts for more than 50%, and the average annual output power is approximately 33% of the installed capacity [16]. If the $N-1$ principle is adopted for an electrical system, it leads to long-term offshore electricity generation under a low load, consequently increasing the design redundancy of the transmission system, and wasting construction, investment, and operation resources of the offshore electrical system.

To determine the required redundancy level, the risk of curtailment of available energy should be decided. This has led to a redundancy of N in many existing wind farms (i.e., sufficiently carry the full load power of the wind farm), and in some circumstances to redundancy N+ "a little bit" (i.e., not enough to carry the full load output of the wind farm). In many cases, this decision has been made heuristically rather than through a quantitative risk assessment of the likelihood that the available energy will need to be curtailed. Hence, the CIGRE Study Committee B3 has developed an offshore electrical system planning method based on the N+ design [17]. The method considers the probability distribution of power generation, availability of wind turbines, and statistical data of component failures. Then, a quantitative risk assessment of offshore substations and transmission system infrastructure is performed. The N+ design is widely recognized by the Crown Estate and DNV GL, the largest offshore wind power developers in the UK. Based on the N+ design, the cost per kWh of electricity is calculated for a 500 MW offshore substation and high-voltage transmission cable of a 540 MW offshore wind farm in the UK [18]. The results show that N+ design can reduce the cost per kWh of electricity for offshore wind farms in a transmission system.

The N+ design reduces the cost by reducing redundancy, giving up part of the electric energy under an overload to select equipment with a smaller capacity [17]. However, the research on electrical system planning based on the N+ design is scarce. Existing electrical system infrastructure configurations based on the N+ design are usually selected according to experience or simple quantitative evaluations, omitting comprehensive evaluation and optimization. Moreover, when the transmission capacity exceeds the rated limit, most systems directly shut down and abandon wind power generation, thus wasting resources.

We propose a method for electrical system planning of large-scale offshore wind farms based on the N+ design and optimized upper power limits of wind turbines. As the N+ design has not been fully evaluated and optimized in electrical system planning, we construct an N+ planning model considering the power-limited operation of wind turbines. In addition, a solution method is devised considering the optimization of the upper power limits of wind turbines under the N+ design. A hybrid algorithm combined with game model is introduced to optimize the investment cost of the electrical system, wind energy loss caused by N+ planning, and electromagnetic interference range. Finally, we optimize the capacity selection of medium- and high-voltage submarine cables and offshore substations in offshore wind farms. Electrical system planning considering 56 wind turbines of 6 MW in an offshore wind farm in China is optimized and analyzed as a representative case study.

II. Mathematical Modeling

This paper presents a method for power system planning based on the N+ design, i.e., the configuration of submarine cables and transformers below the rated capacity of the wind farm, aiming to reduce the initial investment cost of the electrical system [17]. However, offshore wind farms also face various challenges such as wind abandonment and increasing operating loss. We aim to balance economic and environmental requirements. Specifically, to meet the requirements for economic and operational reliability and considering long-term sustainability of the sea life environment complying with the sustainable development of offshore wind power, we quantify the economy, environmental friendliness, and risk of wind abandonment. As a result, we perform electrical system planning that is suited to current large-scale offshore wind power parity development. We establish the following electrical system optimization models based on the N+ design: ① output power model of a single wind turbine; ② wind model; ③ fault model of substation or transmission system; ④ economic model; ⑤ wind abandonment risk model; and ⑥ environmental sustainability model. The following subsections detail these models.

A. Output Power Model of Single Wind Turbine Considering Power-limited Operation

We adopt power-limited operation to consider submarine cables and transformers that exceed the transmission capacity constraint caused by the N+ design. Therefore, the output power of a single wind turbine is determined by the wind condition, wind turbine parameters, and transmission capacity constraints of the electrical system. A binomial form is used to describe the output power of a wind turbine when the wind speed is less than its rated value, and a piecewise function is used to describe the wind speed-power characteristics. The output is given by:

$$P_{wt}(v)=\begin{cases}0 & 0\le v<V_{ci} \text{ or } v>V_{co}\\ P_R(A+Bv+Cv^2) & V_{ci}\le v<V_{r+}\\ P_{R+} & V_{r+}\le v\le V_{co}\end{cases} \tag{1}$$

where P_R is the rated power of a single wind turbine; P_{R+} is the upper power limit of the wind turbine considering the N+ design and is used as the optimization variable of the electrical system; v is the instantaneous wind speed of the installation site of the wind turbine; V_{ci} and V_{co} are the cut-in and cut-out speeds of the wind turbine, respectively; and V_{r+} is the wind speed corresponding to the upper power limit of the wind turbine under the N+ design.

V_{r+} depends on P_{R+} such that V_{r+} can be solved by letting $P_{wt}(v)=P_{R+}$:

$$V_{r+}=\frac{1}{2C}\left[-B+\sqrt{B^2-4C\left(A-P_{R+}/P_R\right)}\right] \tag{2}$$

where binomial parameters A, B, and C correspond to the wind turbine power characteristic curves and are only determined by the turbine design.

B. Wind Model

The wind model is the basis of wind power simulation, being fundamental for analyzing the integration of wind power into a power system [19]. Offshore wind power shows great volatility, and the wind speed distribution widely varies according to the season. To keep the probability distribution and time-series dependence of the original wind speed data, we use a K-order Markov chain to construct a time-series model of wind speed [20], which provides the basis to extract wind resource statistics. The Markov series model is given by:

$$p(v_{t+1}|v_{t-(k-1)},v_{t-(k-2)},...,v_t)=\int_0^{v_{t+1}} f(z|v_{t-(k-1)},v_{t-(k-2)},...,v_t)\mathrm{d}z \tag{3}$$

$$\begin{aligned}P(V_{t+1}\le v_{t+1}|V_t=v_t,V_{t-1}=v_{t-1},...,V_{t-(k-1)}=v_{t-(k-1)},...,V_0=v_0)=\\ P(V_{t+1}\le v_{t+1}|V_t=v_t,V_{t-1}=v_{t-1},...,V_{t-(k-1)}=v_{t-(k-1)})=\\ p(v_{t+1}|v_{t-(k-1)},v_{t-(k-2)},...,v_t)\end{aligned} \tag{4}$$

where $p(v_{t+1}|v_{t-(k-1)},v_{t-(k-2)},...,v_t)$ is the state transition function, representing the probability distribution of state variable V_{t+1} with known states for the first k moments of the stochastic process; and $f(v_{t+1}|v_{t-(k-1)},v_{t-(k-2)},...,v_t)$ is the state transition density function, which can be obtained by the connection function (Copula). More details of the model are available in [20], and the simulated state transitions of Markov series model for wind speed are shown in Fig. 1, where $p_{x,y}$ is the probability of transition from state x to y.

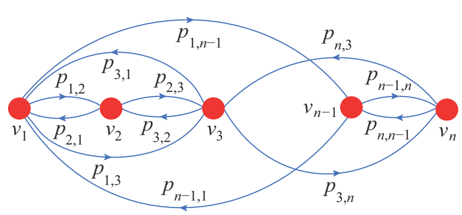

Fig. 1. Simulated state transitions of Markov series model for wind speed.

As the climate of a region can be considered as relatively stable for decades, the wind model in such period remains statistically unchanged [21]. The Weibull distribution is the most commonly used in wind resource statistics [22], [23], and its probability density function (PDF) is given by:

$$PDF(v)=(m/c)(v/c)^{m-1}\exp(-(v/c)^m) \tag{5}$$

where m and c are the scale and shape parameters and can be determined by the maximum likelihood estimation from the data as:

$$m=\left(\frac{\sum_{i=1}^n v_i^m \ln v_i}{\sum_{i=1}^n v_i^m}-\frac{1}{n}\sum_{i=1}^n \ln v_i\right)^{-1} \tag{6}$$

$$c=\left(\frac{1}{n}\sum_{i=1}^n v_i^m\right)^{\frac{1}{m}} \tag{7}$$

where v_i is the i^{th} observed wind speed; and n is the number of wind speed measurements.

C. Fault Model of Substation or Transmission System

To satisfy the $N-1$ requirement, various transformers are usually installed in offshore substations. Under the N+ design, a light offshore substation is often used, and only one transformer should be installed. When transformers are connected, they can be used as backup for another one in case of failure to reduce the possibility of a total shutdown of all the wind turbines at a substation. The schematics of a wind farm with light substations and conventional wind farm are shown in Fig. 2.

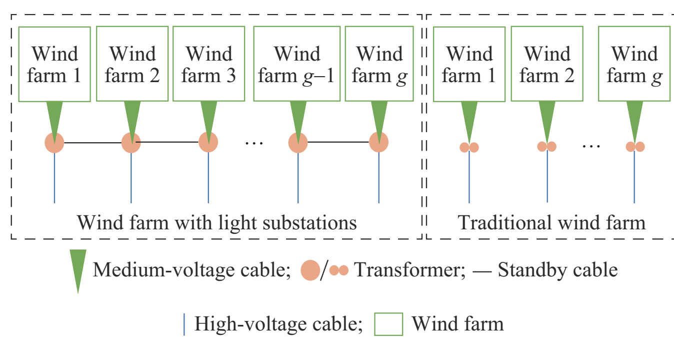

Fig. 2. Schematics of wind farm with light substations and conventional wind farm.

As we establish a difference model, it shows no effect whether the wind speed exceeds the critical point of wind abandonment. Therefore, it is only necessary to add the case when the wind speed exceeds that critical point. Active wind turbine abandonment is important in the N+ design for the selection of submarine cables because the cross-section of cables cannot withstand the electric energy generated by all the wind turbines in two wind farms. Thus, the upper power limit of each wind turbine should be actively controlled, and the wind speed at which active control is switched to no control is the critical point of active wind turbine abandonment. Regional wind farms can be divided into single- and double-standby wind farms. Single-standby wind farms are wind farms 1 and g, as illustrated in Fig. 2. When the substation or high-voltage cable of a single-standby wind farm fails, there is only one standby route. Figure 2 shows only double-standby wind farms excluding the two single-standby wind farms. When a substation or high-voltage cable from a double-standby wind farm fails, two standby routes are available.

When a cable or transformer fails, two situations may occur. First, a whole-area shutdown of all the wind turbines in a wind farm can occur. Alternatively, a partial shutdown of various wind turbines in a wind farm can occur. When a single- or double-standby wind farm experiences a whole-area or partial shutdown, the high-voltage cable, standby cable, and booster station have the operating states listed in Tables I and II, where × indicates failure and √ indicates normal operation.

TABLE I
POSSIBLE SITUATIONS CAUSED BY CABLE OR TRANSFORMER FAILURE IN SINGLE-STANDBY WIND FARM

Situation	Booster station	Standby cable	High-voltage cable	Adjacent high-voltage cable
Whole-area shutdown	×			
	√	×	×	
	√	√	×	×
Partial shutdown	√	√	×	√

TABLE II
POSSIBLE SITUATIONS CAUSED BY CABLE OR TRANSFORMER FAILURE IN DOUBLE-STANDBY WIND FARM

Situation	Booster station	Standby cable 1	Adjacent high-voltage cable1	Standby cable 2	Adjacent high-voltage cable 2	High-voltage cable
Whole-area shutdown	×					
	√	×		×		×
	√	×		√	×	×
	√	√	×	×		×
Partial shutdown	√	√	√	×		×
	√	×		√	√	×

The probability of whole-area shutdown in a single-standby wind farm is given by:

$$P_{salf}=P_{ST}+P_{SH}P_{SB}(1-P_{ST})+P_{SH}P_{SHadj}(1-P_{SB})(1-P_{ST}) \quad (8)$$

where P_{ST} is the probability of transformer failure in a single-standby substation; P_{SH} is the probability of high-voltage cable failure in a single-standby wind farm; P_{SB} is the probability of standby cable failure in a single-standby wind farm; and P_{SHadj} is the probability of high-voltage cable failure in wind farms adjacent to a single-standby wind farm.

The probability of partial shutdown in a single-standby wind farm is given by:

$$P_{sapf}=P_{ST}P_{SH}(1-P_{SB})(1-P_{SHadj}) \quad (9)$$

The probability of whole-area shutdown in a double-standby wind farm is given by:

$$\begin{aligned}P_{Dalf}=&P_{DT}+P_{DH}P_{DB1}P_{DB2}(1-P_{DT})+\\&P_{DH}P_{DHadj2}P_{DB1}(1-P_{DB2})(1-P_{DT})+\\&P_{DH}P_{DHadj1}P_{DB2}(1-P_{DB1})(1-P_{DT})\end{aligned} \quad (10)$$

where P_{DT} is the probability of transformer failure in a double-standby substation; P_{DH} is the probability of high-voltage cable failure in a double-standby wind farm; P_{DB1} and P_{DB2} are the probabilities of standby cable failures of the double-standby wind farm; and P_{DHadj1} and P_{DHadj2} are the probabilities of high-voltage cable failures in wind farms adjacent to the double-standby wind farm.

The probability of partial shutdown in a double-standby wind farm is given by:

$$\begin{aligned}P_{Dalf}=&P_{DH}P_{DB1}(1-P_{DT})(1-P_{DB2})(1-P_{DHadj2})+\\&P_{DH}P_{DB2}(1-P_{DT})(1-P_{DB1})(1-P_{DHadj1})\end{aligned} \quad (11)$$

D. Economic Model

The economy of an electrical system mainly considers the net present value income, ΔNPV, which determines the change in net present value between conventional planning and N+ lectotype planning. ΔNPV involves investment income ΔC_p and energy loss ΔC_{qi}, which is calculated as:

$$\Delta NPV=\Delta C_p-\Delta C_{qi} \quad (12)$$

The investment income ΔC_p includes the initial investment income ΔC_I and operating loss income ΔC_O of an electrical system, as shown in (13). The income means the change in economy between conventional planning and N+ lectotype planning.

$$\Delta C_p=\Delta C_I+\Delta C_O P_{V,sum} \quad (13)$$

where $P_{V,sum}$ is the present value of annual investment expenses given by:

$$P_{V,sum}=[(1+r)^t-1]/[r(1+r)^t] \quad (14)$$

where r is the discount rate, which is generally set to be 8%; and t is the expected service life.

The initial investment income ΔC_I considers the investment expenses of medium- and high-voltage cables and materials and the construction costs of offshore substations:

$$\Delta C_I=\sum_{i=1}^{N_i}(\Delta C_{M,cab}+\Delta C_{inst})+\Delta C_{H,cab}+\Delta C_{sub} \quad (15)$$

where N_i is the number of cable feeders in the wind farms; $\Delta C_{M,cab}$ and ΔC_{inst} are the medium-voltage cable and laying cost incomes, respectively; $\Delta C_{H,cab}$ is the high-voltage cable cost income; and ΔC_{sub} is the offshore substation investment and construction cost income.

As the operating loss of the collector system is small and varies slightly, we neglect its influence. The operating loss income ΔC_O mainly includes the transmission loss income of electric energy in high-voltage cables $\Delta C_{Hcab,o}$ and operating loss income of transformers $\Delta C_{T,o}$ as follows:

$$\Delta C_O=\Delta C_{Hcab,o}+\Delta C_{T,o} \quad (16)$$

The operating loss income of transformer is heuristically estimated by associating the transformer rating with the initial substation capacity and proportional index e. The transmission and operating loss incomes are calculated as [24]:

$$\Delta C_{Hcab,o}=c_1(I_u^2R_u-I_{u+}^2R_{u+})t_H \quad (17)$$

$$\Delta C_{T,o}=-Z_{T,base}[1-(P_{T,+}/P_{T,base})^{scl}] \quad (18)$$

where c_1 is the on-grid price of offshore wind power; I_u and I_{u+} are the root-mean-square currents of the high-voltage submarine cable considering the $N-1$ and N+ designs given by (19) and (20), respectively; R_u and R_{u+} are the resistance values of the high-voltage submarine cable considering the $N-1$ and $N+$ designs, respectively; t_H is the total running time; $Z_{T,base}$ is the annual operating loss cost of the initial substation; $P_{T,base}$ is the initial substation capacity; $P_{T,+}$ is the substation capacity under the $N+$ design; and scl is a scaling index, which is generally set to be 0.8.

$$I_u=\sqrt{\frac{1}{T}\sum_{e=V_{ci}}^{V_{co}} I_e^2 t_e} \tag{19}$$

$$I_{u+}=\sqrt{\frac{1}{T}\left[\sum_{e=V_{ci}}^{V_{r+}} I_e^2 t_e+\sum_{e=V_{r+}}^{V_{co}}\left(\frac{P_{R+}}{\sqrt{3}\,U_{H,rate}}\right)^2 t_e\right]} \tag{20}$$

where I_e is the current generated by wind turbine at wind speed e; $U_{H,rate}$ is the rated voltage of transmission system; t_e is the duration of the corresponding current; and $T=8760$ hours per year.

The calculation of the wind abandonment loss is essential to the lectotype and optimization of offshore transformers and submarine cables under the $N+$ design. The calculation of the abandoned wind loss directly affects the optimal planning result. Energy loss ΔC_{qi} given by (21) mainly comprises two parts. One part is the wind energy resource loss C_{qi1} owing to the limited wind turbine output caused by transmission capacity constraints of electrical equipment considering the $N+$ design. The other is the loss expectation C_{qi2} caused by a reduction in the transmittable capacity of wind power owing to a reduced redundancy when an offshore substation or high-voltage submarine cable in the wind farm partition fails.

$$\Delta C_{qi}=(C_{qi1}+C_{qi2})P_{V,sum} \tag{21}$$

C_{qi1} is obtained considering the probability of wind speed at the location of the wind turbine, as shown in (22); and C_{qi2} is calculated considering the energy loss caused by different operating states of offshore substations and high-voltage submarine cables, as shown in (23).

$$C_{qi1}=c_1 T\sum_{wt\in sub}\int_{V_{r+}}^{V_{co}}(P_{wt}(v)-P_{wt,N+}(v))\cdot PDF(v)\mathrm{d}v \tag{22}$$

$$C_{qi2}=c_1\lambda\rho(P_{h1}t_{h1}\Delta P_{adsub}+P_{h2}t_{h2}\Delta P_{sub,N+}) \tag{23}$$

where $P_{wt,N+}(v)$ is the upper power limit of a wind turbine considering the $N+$ design; $P_{wt}(v)$ is the output power of a wind turbine at the corresponding wind speed v; P_{h1} is the probability of a partial shutdown of a substation in a standby state; t_{h1} is the failure downtime corresponding to P_{h1}; P_{h2} is the probability of a whole-area shutdown of a substation in a standby state; t_{h2} is the failure downtime corresponding to P_{h2}; λ is the simultaneous coefficient of the wind turbine shutdown caused by a submarine cable or transformer fault and wind turbine failure; ρ is the probability of the wind speed exceeding the critical point of wind abandonment; sub is the number set of the wind turbines in the substation; $\Delta P_{sub,N+}$ is the change in capacity between the substations in the $N-1$ and $N+$ designs; and ΔP_{adsub} is the change in capacity between the substations of adjacent wind farms in the $N-1$ and $N+$ designs.

E. Wind Abandonment Risk Model

The risk of wind abandonment involves the wind energy loss caused by the $N+$ design as:

$$P_{qi}=T\sum_{wt\in sub}\int_{V_{r+}}^{V_{co}}(P_{wt}(v)-P_{wt,N+}(v))\cdot PDF(v)\mathrm{d}v \tag{24}$$

F. Environmental Sustainability Model

The environmental sustainability of an electrical system is mainly determined by the electromagnetic interference impact caused by the cable operation as [6]:

$$V=\sum_{s=1}^{N_s}\sum_{f=1}^{N_{sf}}\sum_{c=1}^{N_{sfc}} S_{sfc}L_{sfc}+\sum_{s=1}^{N_s} S_{H,s}L_{H,s} \tag{25}$$

where S_{sfc} and $S_{H,s}$ are the cross-sectional areas of the medium-voltage cable in the C-section submarine cable of the F-series feeder of booster station S and high-voltage cable of booster station S, respectively; and L_{sfc} and $L_{H,s}$ are the lengths of the medium- and high-voltage cables, respectively. The magnetic induction strength exceeds the control limit of 100 μT under the maximum continuous load current.

III. Planning Method Considering Power-limited Operation of Wind Turbines and $N+$ Design

In conventional $N-1$ planning, the medium-voltage submarine cable capacity is generally selected according to the installed capacity of the offshore wind turbines, while the selections of substation and high-voltage submarine cable capacities consider a certain capacity-to-load ratio based on the calculated load, with an approximate capacity-to-load ratio K_C of 1-1.5. The corresponding expressions are given by:

$$K_{M,sfc}I_{M,sfc,o}\geq\frac{\sum_{wt\in sub}P_{wt}}{\sqrt{3}\,U_{M,rate}} \tag{26}$$

$$K_{Hc}I_{H,o}\geq\frac{K_C\sum_{wt\in sub}P_{wt}}{\sqrt{3}\,U_{H,rate}} \tag{27}$$

$$P_{Tsum}\geq K_C\sum_{wt\in sub}P_{wt} \tag{28}$$

where $K_{M,sfc}$ is the overall correction coefficient of the long-term allowable current-carrying capacity; $I_{M,sfc,o}$ is the long-term current-carrying capacity of the medium-voltage cable; K_{Hc} is the overall correction coefficient of the long-term allowable current-carrying capacity; $I_{H,o}$ is the long-term current-carrying capacity of the high-voltage cables; and P_{Tsum} is the capacity of the offshore substation.

Based on the $N+$ design, we consider the power-limited operation of wind turbines to optimize the lectotype of the electrical system infrastructure in offshore wind farms and establish a two-layer optimization model.

A. Outer-layer Model

The outer-layer model is formulated as a multi-objective optimization problem with three objectives to maximize the net present value income, wind energy loss, and electromagnetic interference impact range. The outer-layer model mainly optimizes the lectotype of cables and transformers and provides parameters to the inner model.

The outer-layer model is formulated as:

$$Obj1:\ \max f_1(P)=\Delta NPV \tag{29}$$

$$Obj2:\ \min f_2(P)=P_{qi} \tag{30}$$

$$Obj3:\ \min f_3(P)=V \tag{31}$$

s.t.

$$\begin{cases} I_{Hc,\max+}\le K_{Hc}I_{H,o} \\ S_H\ge S_{H,\min} \\ \left|\Delta U_H\right|\le\left|\Delta U_{H,\max}\right| \\ P_{Tsum}\ge\sum\limits_{wt\in sub}P_{wt,N+} \\ P_{wt,\min}\le P_{wt,N+}\le P_{wt,\max} \end{cases} \tag{32}$$

$$I_{Hc,\max+}=\frac{\sum\limits_{wt\in sub}P_{wt,N+}}{\sqrt{3}\,U_{H,rate}} \tag{33}$$

where $I_{Hc,\max+}$ is the maximum sustained load current flowing through the high-voltage cables considering the N+ design given by (33); S_H is the cross-section of high-voltage cable; $S_{H,\min}$ is the minimum cross-section allowed for high-voltage cable to meet the short-circuit thermal stability standard; ΔU_H is voltage drop of the high-voltage cables; $\Delta U_{H,\max}$ is the maximum allowable voltage drop of the high-voltage cables; $P_{wt,N+}$ is the upper power limit of the wind turbine considering the N+ design used as the optimization variable of the electrical system; $P_{wt,\min}$ is the minimum power of a wind turbine, which is 20% of the rated power [25]; and $P_{wt,\max}$ is the maximum power of a wind turbine. The constraints in (32) are the long-term allowable load capacity, short-circuit thermal stability check, and voltage drop check of the high-voltage cable, as well as the capacity limit of the offshore substation and upper and lower power limits of a single wind turbine.

B. Inner-layer Model

The inner-layer model mainly considers changes in the optimal value of the collector system caused by different upper power limits of wind turbines in the outer model. Also, it takes the minimum topology cost of the collector system as the objective function and iteratively optimizes its topology based on the genetic and minimum spanning tree algorithms.

The inner-layer model is formulated as:

$$Obj:\ \min C_M=\sum_{i=1}^{N_i}(C_{M,cab}+C_{inst}) \tag{34}$$

s.t.

$$\begin{cases} I_{M,sfc,\max+}\le K_{M,sfc}I_{M,sfc,o} \\ S_M\ge S_{M,\min} \\ \left|\Delta U_M\right|\le\left|\Delta U_{M,\max}\right| \\ F_i\cap F_j=\varnothing \quad i,j\in S, i\ne j \\ F_i\cup F_j=S \end{cases} \tag{35}$$

where $I_{M,sfc,\max+}$ is the maximum sustained load current flowing through the C-section submarine cable of the F-series feeder of booster station S considering the N+ design given by (36); H_{sfc} is the set of wind turbines carried by medium-voltage cable sfc; S_M is the cross-section of mediun-voltage cable sfc; $S_{M,\min}$ is the minimum allowed cross-section for medium-voltage cable sfc to meet the short-circuit thermal stability standard; ΔU_M is the voltage drop of the medium-voltage cable sfc; $\Delta U_{M,\max}$ is the maximum allowable pressure drop of the medium-voltage submarine cable; F_i and F_j are the sets of wind turbine nodes; and S is the set of all the wind turbines in a wind farm. The constraints in (35) are the long-term allowable load capacity, short-circuit thermal stability check, and voltage drop check of the medium-voltage submarine cable. The absence of intersection between wind turbine node sets and all the turbines of a wind farm must be included in the turbine node set.

$$I_{M,sfc,\max+}=\frac{\sum\limits_{wt\in H_{sfc}}P_{wt,N+}}{\sqrt{3}\,U_{M,rate}} \tag{36}$$

IV. Game Optimization Solution

Owing to the complexity of multi-objective optimization, only valid solutions to the problem are usually found, and a problem often has various valid solutions. Hence, we introduce a hybrid algorithm combined with a game model to solve the multi-objective optimization model.

A. Game Optimization Model

Considering the emphasis on different indicators for wind farm operation as well as inherent statistical trends and representative values in data, we use the AHP-CRITIC weight method to iteratively optimize the weight assignment of indicators with multiple objectives. Subjective and objective weights are combined and optimized by multiplicative synthesis.

Based on the mixed-strategy Nash equilibrium [26], [27], we select the population with the best comprehensive performance regarding economy, wind abandonment risk, and environmental sustainability across iterations. Populations generated algorithmically constitute strategy set Z of a game model, and player set H is composed of the indicators with multiple objectives. Combining the calculation results of combined weights and considering influence strength W_i among the constituent elements, its payoff function is $u(W_i)$, and the payoff function set is $U=\{u|u_i(W_i\subset H)\}_{n\times m}$. Game optimization is expressed as $G=\{H,Z,U\}$ equivalent to a linear model:

$$\begin{cases} M=\min\sum\limits_{i=1}^{m}y_i \\ \text{s.t. } 1-\sum\limits_{i=1}^{m}a_{ij}y_i\le 0 \quad j=1,2,\ldots,n \\ \quad y_i\ge 0 \quad i=1,2,\ldots,m \end{cases} \tag{37}$$

where y_i represents any mixed strategy of Z based on alternative i; and a_{ij} is a coefficient [6].

B. Optimization Solution to N+ Lectotype and Strategic Decision Considering Optimized Upper Power Limits of Wind Turbines

Heuristic optimization is widely used in many areas [28]. For instance, chaotic hybrid butterfly optimization with particle swarm optimization provides fast convergence and stability for high-dimensional numerical optimization [29]. Accordingly, we introduce a hybrid algorithm combined with a game model to optimize the solution to the N+ lectotype and strategic decision for the target electrical system. The detailed optimization procedure is described in Fig. 3.

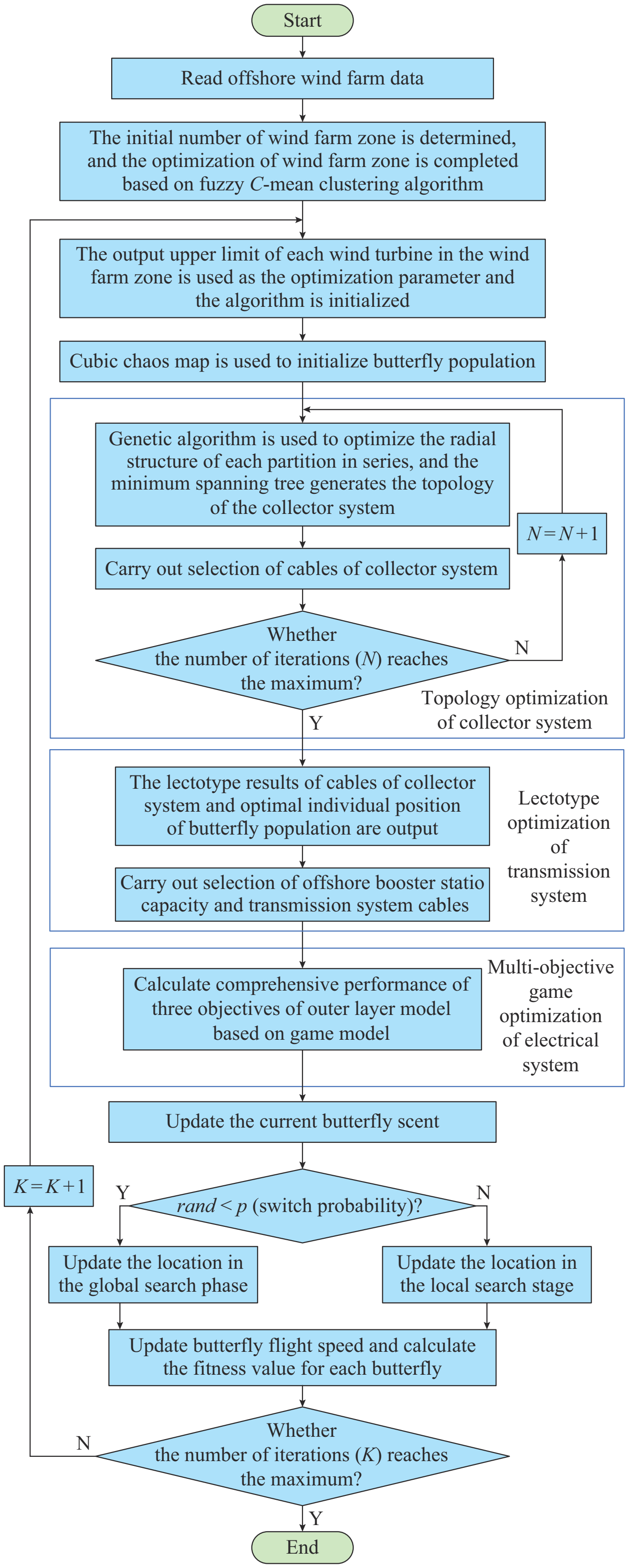

Fig. 3. Flowchart of N+ lectotype game optimization for electrical system based on chaotic hybrid butterfly optimization and particle swarm optimization.

The optimization consists of the following main steps.

Step 1: perform cluster partition of offshore wind farms and determine the location of offshore substations.

Step 2: take the upper power limit of each wind turbine within the wind farm zone as the optimization variable and initialize the hybrid algorithm.

Step 3: take the optimization parameters in the hybrid optimization algorithm as inputs. Minimize the objective function of the inner-layer model, namely, the investment cost of the collecting system. Optimize the topology of the collector system and cable lectotype under different upper power limits of wind turbine using the genetic algorithm.

Step 4: use the optimization results of the collector system as input for the lectotype of offshore substations and power transmission systems.

Step 5: iteratively apply the game model to optimize the multi-objective solution of the outer-layer model.

V. Case Study

A. Case Description

We have evaluated an offshore wind farm with capacity of 336 MW and optimized the lectotype of cables and transformers in the electrical system. The wind farm contained 56 wind turbines of 6 MW. The distribution of the wind turbines and locations of onshore substations are shown in Fig. 4.

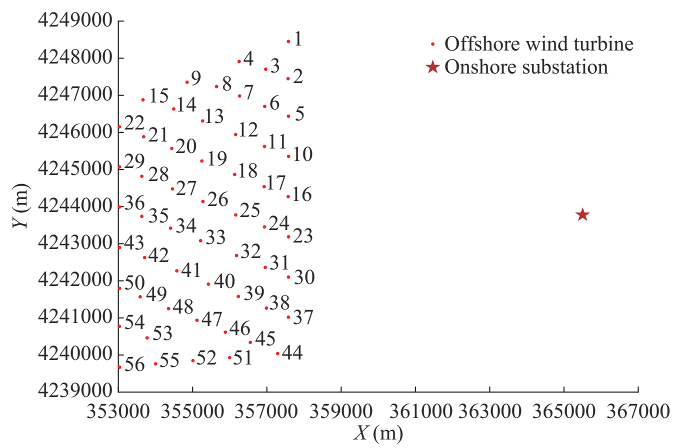

Fig. 4. Distribution of wind turbines and locations of onshore substations.

The voltage level of the medium-voltage cable is 35 kV, and that of the high-voltage cable is 220 kV. The service life of the offshore wind farm is 20 years. The failure rate of both the high-voltage and standby cables is 0.045 time/(km·year), and their repair time is 1000 hours. The failure rate of the offshore transformer is 0.02 time/year, and its repair time is 200 hours [5], [6].

The probability distribution of the historical wind speed for the evaluated wind farm is shown in Fig. 5. The wind speed followed a Weibull distribution.

B. Analysis of Planning Results

The electrical system equipment lectotype of offshore wind farms is currently based on $N-1$ principle (reference).

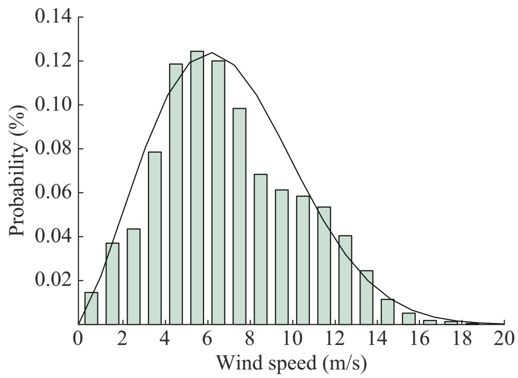

Fig. 5. Probability distributon of historical wind speed for evaluated wind farm.

The *N*+ lectotype planning (baseline) only selects and optimizes the capacity of the transmission system and offshore substations of offshore wind farms, but the selection and optimization of the cable capacity of the collector system are not performed. Hence, we propose *N*+ lectotype planning with game optimization based on a heuristic algorithm to optimize the upper power limit of each wind turbine while considering the power-limited operation of wind turbines. We compared this method with *N*+ planning that considers the power-limited operation of wind turbines but not the output ceiling optimization, i. e., the best upper power limit of a wind turbine is selected based on enumeration under the same output ceiling across wind turbines.

The lectotype of the submarine cables and transformers in the electrical system has been optimized, and four planning methods are analyzed and compared, which are conventional $N-1$ planning, baseline *N*+, *N*+ planning with and without output optimization. The lectotype results of the submarine cables and transformers in the electrical systems and topologies of the collector systems obtained from the evaluated planning schemes are shown in Fig. 6(a)-(d).

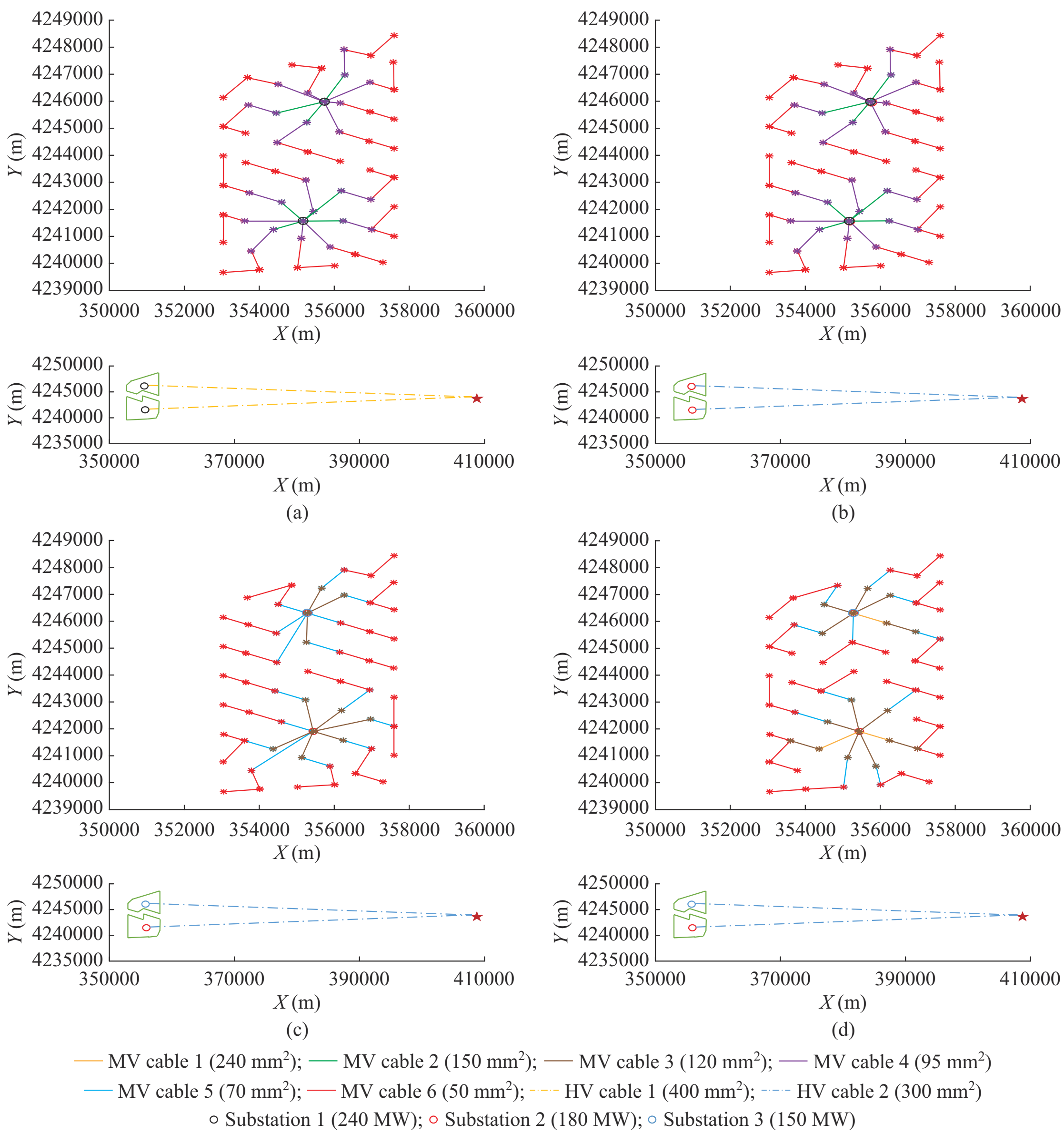

Fig. 6. Schematic of lectotype results of submarine cable and offshore booster station in electrical system using different methods. (a) Conventional $N-1$ planning. (b) Baseline *N*+ planning. (c) *N*+ planning with output optimization. (d) *N*+ planning without output optimization.

The upper power limits of the wind turbines in N+ planning with and without output optimization are shown in Fig. 7.

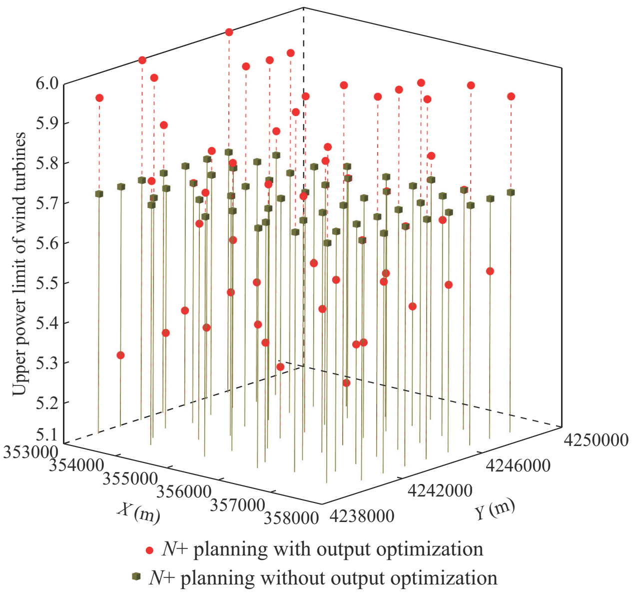

Fig. 7. Upper power limits of wind turbines in N+ planning with and without output optimization.

Results of the electrical system infrastructure lectotype for the evaluated planning methods are shown in Fig. 8.

The planning results show that compared with conventional $N-1$ planning, the cable cross-section and substation capacity are reduced when using the baseline N+ planning and N+ planning with and without output optimization. N+ planning with output optimization provides the smallest cable cross-section, indicating an economic advantage.

C. Economic Analysis

The costs of electrical systems with different planning methods are listed in Table III. Table III shows that with the optimization of the capacities of offshore transformers and cables, N+ planning with output optimization provides the best economic benefits. Compared with conventional $N-1$ planning, the initial investment cost of the baseline N+ planning is reduced by 13.44%, while that of N+ planning without output optimization is reduced by 14.18%, and that of N+ planning with output optimization is reduced by 14.32%. The reduction in the initial investment cost by using N+ planning with output optimization is mainly due to the transmission system, while the investment cost reduction by the current collection system is relatively small, being approximately 6%.

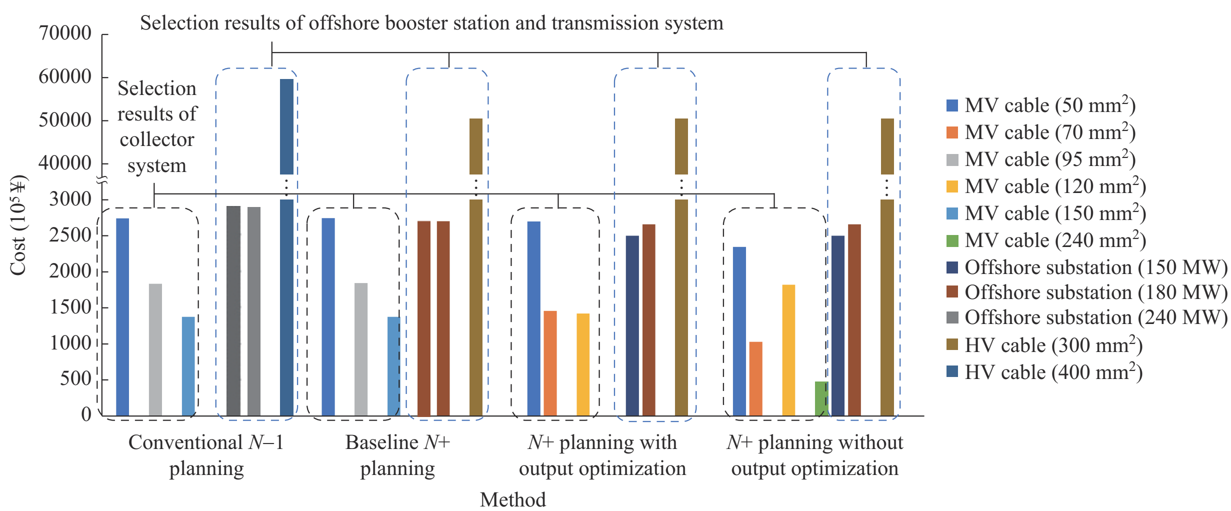

Fig. 8. Results of electrical system infrastructure lectotype.

TABLE III
COSTS OF ELECTRICAL SYSTEMS WITH DIFFERENT PLANNING METHODS

Planning method	Cost (10^4 ¥)				
	Collector system	Offshore booster station	Power transmission system	Operating loss	Wind energy loss
Conventional $N-1$	5960.43	5788	59730	12612.58	7119
Baseline N+	5960.43	5402	50500	14435.34	8560
N+ planning with output optimization	5574.52	5161	50500	14958.31	8092
N+ planning without output optimization	5669.13	5161	50500	14911.87	8216

D. Comprehensive Analysis of Planning Methods

The four planning methods are compared and analyzed based on the mixed-strategy Nash equilibrium and solved based on the path tracking algorithm, whose solution is detailed in [26]. The evaluation indices of the compared planning methods are listed in Table IV.

Table VI shows that N+ planning with output optimization is the best planning method with the highest overall performance. Compared with conventional $N-1$ planning, N+ planning with output optimization improves the economic benefit by 7.6% and reduces the electromagnetic interference impact by approximately 10% and the annual available capacity of wind farms by 5.5%.

TABLE IV
EVALUATION INDICES OF DIFFERENT PLANNING METHODS

Planning method	Cost (10^4 ¥)	Environment-friendly (m^3)	Wind abandonment risk (MW)
Conventional $N-1$	91202.87	83719.8	8520.88
Baseline *N*+	84857.77	81153.5	9880.43
N+ planning with output optimization	84285.65	75619.8	9690.45
N+ planning without output optimization	84458.00	77542.1	9840.31

N+ planning without output optimization improves the economic benefit by 7.4% and reduces the electromagnetic interference impact by approximately 7% and average annual available capacity of the wind farm by 4.6%. In terms of wind energy utilization, compared with the baseline *N*+ planning, the wind energy losses of *N*+ planning with and without output optimizations are reduced by 1.9% and 0.4%, respectively.

We have also analyzed the computational performance of the proposed *N*+ planning and conventional $N-1$ planning. The convergence curves of the fitness function for conventional $N-1$ planning and *N*+ planning with output optimization are shown in Fig. 9. The *N*+ planning with output optimization reaches the optimal solution at the 172nd iteration, while the conventional $N-1$ planning reaches the optimal solution at the 152nd iteration. Although the *N*+ planning with output optimization converges slower than the conventional $N-1$ planning, the former has a better performance regarding economic indicators, wind abandonment risk, and environmental sustainability.

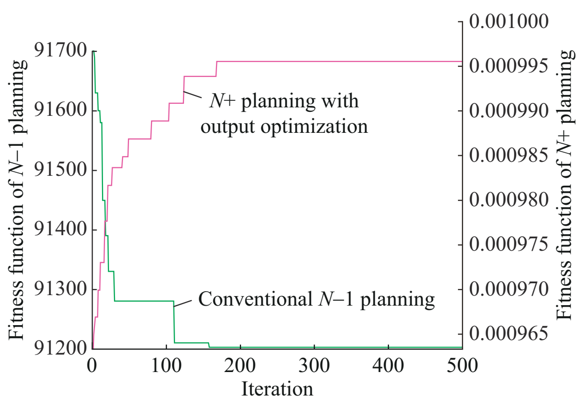

Fig. 9. Convergence curves of conventional $N-1$ planning and *N*+ planning with output optimization.

VI. CONCLUSION

1) For electrical system planning considering the power-limited operation of wind turbines and optimizing the output ceiling of each wind turbine in offshore wind farms, we propose an electrical system planning method considering the *N*+ planning. It solves the limitation of the current *N*+ planning, in which the quantitative evaluation of the integrated equipment lectotype in an electrical system is difficult to perform in practice.

2) The *N*+ lectotype optimization considering the optimization of the upper power limits of wind turbines is performed. The wind energy loss after *N*+ planning in wind farms is reduced by 1.9%, and the life cycle cost of the electrical system is reduced by 7.6%.

3) In the case study, the optimization improvement of transmission systems and offshore substations has reached up to 15.4% and 10.8%, respectively. Although the cost optimization of the collector systems is relatively small, the reduction has reached 6.3%. As the number and capacity of wind turbines in offshore wind farms increase, the economy of planning considering the *N*+ planning will also increase along with the optimization space of the collector system.

4) A hybrid algorithm including a game model is introduced to perform game optimization of the multi-objective model and improves the comprehensive performance of *N*+ planning. Nevertheless, *N*+ planning with output optimization can face difficulties in finding the optimal solution owing to its high dimensionality, which should be addressed in future work.

REFERENCES

[1] J. González, M. Payán, and J. Santos, "A new and efficient method for optimal design of large offshore wind power plants," *IEEE Transactions on Power Systems*, vol. 28, no. 3, pp. 3075-3084, Apr. 2013.
[2] O. Dahmani, S. Bourguet, M. Machmoum *et al.*, "Optimization and reliability evaluation of an offshore wind farm architecture," *IEEE Transactions on Sustainable Energy*, vol. 8, no. 2, pp. 542-550, Apr. 2017.
[3] W. Wang, Y. Qiao, F. Dou *et al.*, "Optimization of offshore wind farm collector systems based on improved genetic algorithm," *Electric Power*, vol. 52, no. 1, pp. 63-68, Jan. 2019.
[4] J. Shin and J. Kim, "Optimal design for offshore wind farm considering inner grid layout and offshore substation location," *IEEE Transactions on Power Systems*, vol. 32, no. 3, pp. 2041-2048, May 2017.
[5] Y. Chen, Z. Dong, K. Meng *et al.*, "A novel technique for the optimal design of offshore wind farm electrical layout," *Journal of Modern Power Systems and Clean Energy*, vol. 1, no. 3, pp. 254-259, Dec. 2013.
[6] Y. Fu, S. Yang, S. Wei *et al.*, "Game based topology optimization for power collection system of large-scale offshore wind farm considering electromagnetic environment constraints," *Automation of Electric Power Systems*, vol. 43, no. 3, pp. 201-208, Jan. 2019.
[7] Z. Jiang, Q. Yu, L. Li *et al.*, "Expansion planning method of offshore multiplatform power system with wind power considering cable size selection," *IEEE Access*, vol. 9, pp. 129796-129809, Sept. 2021.
[8] S. Tao, Q. Xu, A. Feijóo *et al.*, "Joint optimization of wind turbine micrositing and cabling in an offshore wind farm," *IEEE Transactions on Smart Grid*, vol. 12, no. 1, pp. 834-844, Jan. 2021.
[9] L. Wang, J. Wu, Z. Tang *et al.*, "An integration optimization method for power collection systems of offshore wind farms," *Energies*, vol. 12, no. 20, pp. 3965-3965, Oct. 2019.
[10] Y. Yuan, B. Wu, Z. Li *et al.*, "Flexible planning of transmission system with large wind farm based on multi-scenario probability," *Electric Power Automation Equipment*, vol. 29, no. 10, pp. 8-12, Oct. 2009.
[11] J. Zhou, Y. Yu, and Y. Zeng, "Heuristic optimization algorithm for transmission network expansion planning with large-scale wind power integration," *Automation of Electric Power Systems*, vol. 35, no. 22, pp. 66-70, Nov. 2011.
[12] Y. Wu, B. Zhang, L. Yan *et al.*, "Research and modeling of evolutionary game based selection of investment strategies for offshore wind farm," *Power System Technology*, vol. 38, no. 11, pp. 2978-2985, Nov. 2014.
[13] L. Lu, "Research on investment decision-making of offshore wind power construction projects based on interval-valued intuitionistic fuzzy sets," M.S. thesis, Department of Management Science and Engineering, North China Electric Power University, Beijing, China, 2017.
[14] L. Gan, Z. Wu, J. Gu *et al.*, "A MILP model for grid-connection transmission system planning of wind farm clusters," *Transactions of Chi-*

na Electrotechnical Society, vol. 32, no. 5, pp. 165-175, Mar. 2017.

[15] AEMO. (2021, Jun.). AEMO energy generation data. [Online]. Available: https://anero.id/energy/wind-energy

[16] J. Reyes, M. Oliva, A. Prieto *et al.*, "Compact transformers for offshore wind power plants applications," in *Proceedings of 2014 International Conference on Renewable Energies and Power Quality*, Cordoba, Spain, Apr. 2014, pp. 588-593.

[17] J. S. Finn, J. MacEnri, R. Szewczyk *et al.*, "Guidelines for the design and construction of AC offshore substations for wind power plants," WG B3.26, No. 978-2-85873-174-9, Dublin, Ireland, Dec. 2011.

[18] R. Clay, "Sharing lessons learned and good practice in offshore transmission," Tech. Rep. 112843-UKBR-R-01-F, DNV GL, London, UK, Jun. 2014.

[19] K. Xie, Q. Liao, H.-M. Tai *et al.*, "Non-homogeneous Markov wind speed time series model considering daily and seasonal variation characteristics," *IEEE Transactions on Sustainable Energy*, vol. 8, no. 3, pp. 1281-1290, Jul. 2017.

[20] J. Bi, "Wind speed simulation model of wind farm for Yantai area," M.S. thesis, Department of Electric Engineering, Shandong University, Shandong, China, 2019.

[21] P. Jiang, Y. Huo, L. Zhang *et al.*, "A wind time series model based on advanced first-order Markov chain approach," *Automation of Electric Power Systems*, vol. 38, no. 19, pp. 22-27, Oct. 2014.

[22] B. Hicham, E. A. Ikram, E. B. Abdelmajid *et al.*, "Wind speed data analysis using Weibull and Rayleigh distribution functions, case study: five cities northern Morocco," *Procedia Manufacturing*, vol. 32, pp. 786-793, Apr. 2019.

[23] Z. R. Shu and M. Jesson, "Estimation of Weibull parameters for wind energy analysis across the UK," *Journal of Renewable and Sustainable Energy*, vol. 13, no. 2, pp. 1-18, Mar. 2021.

[24] S. H. H. Kazmi, T. Laneryd, K. Giannikas *et al.*, "Cost optimized dynamic design of offshore wind farm transformers with reliability and contingency considerations," *International Journal of Electrical Power & Energy Systems*, vol. 128, p. 106684, Jun. 2021.

[25] Y. Xiao and G. He, "Power-limited operation characteristic analysis and optimal scheduling for large scale wind turbines," *Automation of Electric Power Systems*, vol. 38, no. 20, pp. 18-25, Oct. 2014.

[26] T. Yang and R. Liu, "Safety cost optimization of wind farm project based on game model," *Electric Power*, vol. 42, no. 4, pp. 424-429, Apr. 2021.

[27] R. Gibbons, *A Primer in Game Theory*. London: Pearson Academic, 1992, pp. 29-33.

[28] P. Hou, J. Zhu, K. Ma *et al.*, "A review of offshore wind farm layout optimization and electrical system design methods," *Journal of Modern Power Systems and Clean Energy*, vol. 7, no. 5, pp. 975-986, Sept. 2019.

[29] M. Zhang, D. Long, T. Qin *et al.*, "A chaotic hybrid butterfly optimization algorithm with particle swarm optimization for high-dimensional optimization problems," *Symmetry*, vol. 12, no. 11, pp. 2073-8994, Oct. 2020.

Shurong Wei received the B.S. degree from Northeast Electric Power University, Jilin, China, in 2002, the M.S. degree from Hohai University, Nanjing, China, in 2005, and the Ph.D. degree from Shanghai University, Shanghai, China, in 2016. She is currently a Professor with the Shanghai University of Electric Power, Shanghai, China. Her research interests include offshore wind farm planning and design, fault diagnosis, and operation maintenance.

Hao Wang received the B. S. degree in electrical engineering from the Shaanxi University of Technology, Xi'an, China, in 2020. He is currently working toward the M.S. degree in electrical engineering with the Electrical Engineering College, Shanghai University of Electric Power, Shanghai, China. His research interests include offshore wind farm planning and optimization.

Yang Fu received the M.S. degree from Southeast University, Nanjing, China, in 1993, and the Ph.D. degree from Shanghai University, Shanghai, China, in 2007. He is currently a Professor with Electrical Engineering College, Shanghai University of Electric Power, Shanghai, China. His research interests include power system analysis and new energy planning and optimization.

Fangxing Li received the B.S.E.E. and M.S.E.E. degrees from Southeast University, Nanjing, China, in 1994 and 1997, respectively, and the Ph.D. degree from Virginia Tech, Blacksburg, USA, in 2001. He is currently the James W. McConnell Professor with the EECS Department, University of Tennessee, Knoxville, USA. His current research interests include renewable energy integration, demand response, electricity markets, distributed generation, measurement-based technology, and power system computing.

Lingling Huang received the M.S. degree from Zhejiang University, Hangzhou, China, in 2006, and the Ph. D. degree from Shanghai University, Shanghai, China, in 2018. Currently, she is a Professor with Shanghai University of Electric Power, Shanghai, China. Her research interests include offshore wind farm planning and operation maintenance.